Proceedings – 23rd Annual Conference – IEEE/EMBS Oct.25-28, 2001, Istanbul, TURKEY

Multimodal Integration of High Resolution EEG and Functional Magnetic Resonance: a Simulation Study

Fabio Babiloni[1], Claudio Babiloni[1,2] Filippo Carducci[1,2], Leonardo Angelone[1], Cosimo Del Gratta[3], Gian Luca Romani[3], Paolo Maria Rossini[2], and Febo Cincotti[4]

[1] Dip. Fisiologia umana e Farmacologia, Università "La Sapienza", Rome, [2] "AFAR", Ospedale Isola Tiberina,Rome, ITALY, [3] ITAB, Univ. "Gabriele D'Annunzio", Chieti, ITALY, [4]IRCCS Fondazione Santa Lucia, Rome, ITALY

Abstract- **In this simulation study, we would like to address some questions related to the use of fMRI a priori constraints in the estimation of the cortical source current density. Namely, we would like to assess the utility to include information as estimated from event-related and block-design fMRI, by using as the dependent variable the correlation between the imposed and the estimated waveforms at the level of cortical region of interests (ROI). A realistic head and cortical surface model was used. Factors used were i) the signal to noise ratio of the scalp simulated data (SNR); ii) the particular inverse operator used to estimate the cortical source activity from the simulated scalp data (INVERSE); iii) the strength of the fMRI priors in the estimation of the current activity (K). Analysis of Variance (ANOVA) results revealed that all the considered factors (SNR, INVERSE, K) significantly afflicts the correlation between the estimated and the simulated cortical activity. For the ROIs analyzed in which a presence of fMRI hotspots were simulated, it was observed that the best estimation of cortical source currents were performed with the inverse operator that use the event-related fMRI information. When the ROI analyzed do not present fMRI hotspots, both minimum norm and fMRI-based inverse operators return statistically equivalent correlation values. Such results open the avenue for the use of fMRI-based inverse operator in the estimation of cortical current strengths from motor and cognitive task in the human brain.**

I. Introduction

Electroencephalography (EEG) is an useful technique for the study of brain dynamics and functional cortical connectivity, due to their high temporal resolution (milliseconds;[1]). EEG reflects the activity of cortical generators oriented both tangentially and radially with respect to the scalp surface. However, the different electrical conductivity of brain, skull, and scalp markedly blurs the EEG potential distributions and makes the localization of the underlying cortical generators problematic. Neural sources of EEG can be localized by making a priori hypothesis on their number and extension. When the EEG activity is mainly generated by a known number of cortical sources (i.e. short-latency evoked potentials), the location and strength of these sources can be reliably estimated by the dipole localization technique. However, it is well known that except for the early processing of sensory responses, event-related cortical responses include a distributed network of several and unknown areas. When distributed cortical network is supposed to be active, cortical sources of EEG data should be modeled by linear inverse estimation. With this approach, thousands of equivalent current dipoles are used as a source model and realistic head models reconstructed from magnetic resonance images serve as volume conductor medium [2].

The solution space (i.e. the set of all possible combinations of the cortical dipoles' strengths) is generally reduced by using geometrical constraints. For example, the dipoles can be disposed along the reconstruction of cortical surface with a direction perpendicular to the local surface. An additional constraint is to force the dipoles to explain the recorded data with a minimum or a low amount of energy (minimum-norm solutions). The solution space can be further reduced by using information deriving from hemodynamic measures recorded during the same task [3]. The rationale of a multimodal approach is that neural activity generating EEG potentials increases glucose and oxygen demands [4]. This results in an increase in the local hemodynamic response that can be measured by functional magnetic resonance images (fMRI). Hence, fMRI responses and cortical sources of EEG data can be spatially related. Determination of the priors in the resolution of the linear inverse problem was performed with the use of information from the hemodynamic responses of the cortical areas as revealed by block-design (strength of activated voxels) and by event-related (coupling of activated voxels) fMRI. It is worth of notice that using the block-design fMRI priors for the estimation of current strengths we failed to take into account information about the coupling of the neural sources. This because we use only the information about the presence or absence of a particular source in the set of those whose hemodynamic responses have been elicited by the considered task. However, we take advantage from the hemodynamic responses of the event-related fMRI, in which the time course of the source responses is also available, to estimate the hemodynamic correlation of the neural sources. This estimate is obtained by computing the cross-correlation on the hemodynamic waveforms obtained by the averaged fMRI activity in the analyzed region of interest.

While the effects and the level of the inclusion of block-design fMRI priors in the estimation of source current density has been investigated through simulation studies [3,5] no studies have been yet addressed similar issues for the inclusion of the event-related fMRI priors in the linear inverse problem. In this simulation study, we would like to address some questions related to the use of fMRI a priori constraints in the estimation of the cortical source current density. Namely, we would like to assess the utility to include information as estimated from event-related and block-design fMRI, by using the capacity to recover the imposed simulated cortical activation in different region of interest of a realistic cortical surface model. This was assessed by using as the dependent variable the correlation values between the estimated and the generated waveforms at the cortical level. Factors used are the noise superimposed to the scalp recorded data (with different levels), the inclusion or not of the fMRI priors for the estimation of cortical activity (using weighted minimum norm solutions as well as block and event-related design for the inclusion of fMRI priors), and the level of the tuning parameters for the a priori fMRI-based cortical source

Report Documentation Page

Report Date	Report Type	Dates Covered (from... to)
25OCT2001	N/A	-

Title and Subtitle Multimodal Integration of High Resolution EEG and Functional Magnetic Resonance: a Simulation Study	**Contract Number**
	Grant Number
	Program Element Number
Author(s)	**Project Number**
	Task Number
	Work Unit Number
Performing Organization Name(s) and Address(es) Dip. Fisiologia umana e Farmacologia, Università "La Sapienza", Rome	**Performing Organization Report Number**
Sponsoring/Monitoring Agency Name(s) and Address(es) US Army Research, Development & Standardization Group (UK) PSC 802 Box 15 FPO AE 09499-1500	**Sponsor/Monitor's Acronym(s)**
	Sponsor/Monitor's Report Number(s)

Distribution/Availability Statement
Approved for public release, distribution unlimited

Supplementary Notes
Papers from the 23rd Annual International Conference of the IEEE Engineering in Medicine and Biology Society, 25-28 Oct 2001, held in Istanbul, Turkey. See also ADM001351 for entire conference on cd-rom., The original document contains color images.

Abstract

Subject Terms

Report Classification unclassified	**Classification of this page** unclassified
Classification of Abstract unclassified	**Limitation of Abstract** UU

Number of Pages
4

estimation. Simulations are performed with realistic head and cortical models derived from a normal, healthy subject.

.

II. METHODOLOGY

A. Head and cortical models

For the simulation purposes, we used a subject's multi-compartment head model (scalp, skull, dura mater, cortex) constructed from MRIs. Such model reproduced scalp, skull, and dura mater surfaces with about 1000 triangles for each surface. Source models were built with the following procedure: (i) the voxels belonging to the MR volume of the cortex were selected with a semiautomatic procedure (threshold algorithm); (ii) these points were triangulated obtaining a fine mesh with about 100,000 triangles; (iii) a coarser mesh was obtained by resampling the one described above down to about 3,000 triangles, taking care that the general features of the neocortical envelope were well preserved especially in correspondence of pre- and post-central gyri and frontal mesial area; (iv) an orthogonal unitary equivalent current dipole was placed in each node of the triangulated surface, with direction parallel to the vector sum of the normals to the surrounding triangles. One hundred and twenty-eight electrodes real scalp electrodes position measured by a 3D digitizer on the same subject during an high resolution EEG recording were used during this simulation.

B. Estimation of cortical source current density.

Taking into account the measurement noise, an estimate of the dipole source configuration that generated a measured potential can be obtained by solving the linear system:

$$\mathbf{Ax} + \mathbf{n} = \mathbf{b} \tag{1}$$

where **A** is the lead field matrix, in which each j-th column describes the potential distribution generated on the scalp electrodes by the j-th unitary dipole, **b** is the vector of the recorded potential values, and **n** is the measurement noise, supposed to be normally distributed. The electrical lead field matrix **A** and the data vector **b** must be referenced consistently. Among the several equivalent solutions for the underdetermined system (1), the solution was chosen that satisfies the following variational problem for the sources **x** :

$$x = \arg\min_{x} \left(\|\mathbf{A}x - b\|_{\mathbf{M}}^2 + l^2 \|x\|_{\mathbf{N}}^2 \right) \tag{2}$$

where **M**, **N** are the matrices associated to the metrics of the data and of the source space, respectively. The solution of the variational problem depends on adequacy of the data and source space metrics. Under the hypothesis of **M** and **N** positive definite, the solution of (2) is given by computing the pseudoinverse matrix **G** according to the following expressions:

$$\hat{\mathbf{i}} = \mathbf{Gb}, \quad \mathbf{G} = \mathbf{N}^{-1}\mathbf{A}'\left(\mathbf{A}\mathbf{N}^{-1}\mathbf{A}' + l\mathbf{M}^{-1}\right)^{-1} \tag{3}$$

An optimal regularization of this linear system was obtained by the L-curve approach. This curve, which plots the residual norm versus the solution norm at different λ values, was used to choose the optimal amount of regularization in the solution of the linear inverse problem. Computation of the L-curves and optimal λ correction values was performed with the original Hansen's routines. The metric **M**, characterizing the idea of closeness in the data space, can be particularized by taking into account the sensors noise level by using the Mahalanobis distance. The source metric **N**, can be particularized by taking into account the information from the hemodynamic responses of the single voxels as derived from fMRIs as showed in the following section.

C. Functional hemodynamical coupling constraints.

We present two characterizations of the source metric N that can provide the basis for the inclusion into the linear inverse estimation of the information about the statistical hemodynamic activation of i-th cortical voxels. The first characterization of the source metric N takes into account all the cortical voxels on the basis of their electrical "closeness" to the EEG sensors (column norm normalization). In this case, the inverse of the resulting source metric is

$$\left(\mathbf{N}^{-1}\right)_{ii} = \left\|\mathbf{A}_{\cdot i}\right\|^{-2} \tag{4}$$

in which $(\mathbf{N}^{-1})_{ii}$ is the *i*-th element of the inverse of the diagonal matrix **N** and $\|\mathbf{A}_j\|$ is the L2 norm of the *i*-th column of the lead field matrix **A**. Introducing fMRI priors into the linear inverse estimation produces a bias in the solution: statistically significantly activated fMRI voxels, which are returned by the so called percentage change approach are weighted to account for the EEG measured potentials. The inverse of the resulting metric is

$$\left(\mathbf{N}^{-1}\right)_{ii} = g(a_i)^2 \left\|\mathbf{A}_{\cdot i}\right\|^{-2} \tag{5}$$

in which $(\mathbf{N}^{-1})_{ii}$ and $\|\mathbf{A}_j\|$ has the same meaning described above. The $g(\alpha_i)$ is a function of the statistically significant percentage increase of the fMRI signal assigned to the i-th dipole of the modeled source space. This function was expressed as

$$g(\alpha_i)2 = 1 + (K\text{-}1)\,(\alpha_i / \max(\alpha_l)), \quad K \geq 1,\ \alpha_i \geq 0 \tag{6}$$

where α_i is the percentage increase of the fMRI signal during the task state for the *i*-th voxel and the factor *K* tunes fMRI constraints in the source space. Fixing $K = 1$ let us disregard fMRI priors, thus returning to a purely electrical solution; a value for $K >> 1$ allows only the sources associated with fMRI active voxels to participate in the solution. It was shown that a value for *K* in the order of 10 (90% of constraints for the fMRI information) is useful to avoid mislocalization due to overconstrained solutions. In the following the estimation of the cortical activity obtained with this metric will be denoted as diag-fMRI. The previous definition of the source metric **N** results in a matrix in which

the off-diagonal elements are zero (diag-fMRI). Now, we take advantage of the off-diagonal elements of the matrix **N** to insert the information about the functional coupling about the cortical sources. In particular we set the generic *ij* entry of the inverse of matrix **N**

$$\left(\mathbf{N}^{-1}\right)_{ij} = g(a_i)g(a_j)\left\|\mathbf{A}_{\cdot i}\right\|^{-1}\left\|\mathbf{A}_{\cdot j}\right\|^{-1} \cdot corr_{ij} \qquad (7)$$

where $\|\mathbf{A}_j\|$ and $g(\alpha_i)$ have the same meaning described above and $corr_{ij}$ is the degree of functional coupling between the source *i* and the source *j* during the particular task analyzed as revealed by the correlation of their hemodynamic responses obtained by the event-related fMRI data. In the following the estimation of the cortical activity obtained with this metric will be denoted as corr-fMRI. It is of interest that in the case of uncorrelated sources ($corr_{ij} = 0$, $i \neq j$; $corr_{ii} = 1$), the corr-fMRI formulation leads back to the diag-fMRI one.

D. Regions of interest.

Seven cortical regions of interest (ROIs) were drawn on the computer-based cortical reconstructions by two independent and expert neuroradiologists. Such ROIs will be those related to the primary sensorimotor (S1 and M1) areas both in the ipsilateral and in the controlateral part of the performed movement, as well as supplementary motor area (SMA). Furthermore, ROIs from posterior parietal areas (PP; including at large Broadmann areas, 5,7,39,40,43) were also considered.

E. Distribution of fMRI activated dipoles along the ROIs.

Three of the seven ROIs analysed were chosen as site for the fMRI activations. Such ROIs were these modelling the left S1 and M1 as well as the SMA. In these regions, fMRI activations were regularly distributed. Hence, each j-th entry of the **N** matrix of a dipole belonging to such ROI will be associated with a prefixed $g(\alpha j)$ value, according to (7). Values of $corr_{ij} = 0.85$ have been taken for all dipole pairs belong to the same ROIs, while values of $corr_{ij} = 0.6$ have been taken for the dipole pairs belong to different ROIs. These values were taken as representative by the mean correlation level of the hemodynamic responses in real event-related fMRI acquisition related to voluntary movements.

F. Experimental design.

The experimental design was drawn as follows: 1) to all dipoles belonging to a particular selected ROI it was assigned an equal moment strength, oscillates between 0 and 1 with a square law; 2) all the possible sequences for activating the seven selected ROIs have been considered. A total of 128 trials were generated, each one of 32 data points; 3) through the electric lead field matrix, such cortical oscillation were propagated toward via the realistic volume conductor to the simulated 128 electric sensors, to produce separate HREEG data sets. 4) white noise were added to these datasets, with different levels of signal-to-noise ratios (SNRs; infinity, 30, 20, 10, 5, 3, 1), recalling the typical range of SNR commonly encountered in evoked, cognitive and motor-related tasks; 5) the inverse electric operators described below were applied to these datasets and the consequent cortical activity were estimated in each ROI. Six types of weights for the inverse operators have been used: the minimum norm estimate (MN), the column normalized minimum norm estimate (WMN), the block-design fMRI constraint without and with the column normalization (diag-fMRI and diag-fMRI NC), and the event-related fMRI constraint without and with column normalization (corr-fMRI and corr-fMRI NC); 6) the estimated current source density for each ROI was the average of the current estimates of each dipoles belonging to such ROI; 7) the adequacy of the reconstructed cortical activity were analyzed by computing the correlation at the ROI level between the generated and the estimated activities along all the simulated trials.

G. Statistical analysis.

The obtained results were subjected to the Analysis of Variance (ANOVA). The dependent variable was the correlation between the generated and simulated current density estimation for each region analyzed. The main factors of the ANOVA was the SNR (with seven levels), the type of inverse operator used (with and without fMRI constraints, with six levels) denoted as INVERSE, the value of K parameter for the fMRI-based inverse operator (with four levels; 3, 5, 7, 10), denoted as K. The correction of Greenhouse-Gasser for the violation of the spherical hypothesis in the ANOVA was used. The post hoc analysis was performed with the Scheffe's test.

III. RESULTS

A. Left S1 region

Results for this cortical region are here reported as paradigmatic for all the ROIs with fMRI activations used in this simulation (like left M1, and SMA). All the considered factors (SNR, INVERSE, K) decrease significantly in the simulations the variance of the correlation between the estimated and the computed cortical current densities. F values for SNR ($F = 61.86$, $p < 0.0001$), INVERSE ($F = 3.67.3$, $p< 0.0028$) and K ($F = 6.6$, $p < 0.0002$) are all above the significant threshold of $p = 0.05$. Almost all the interactions between the main factors were statistically significant. F values for K x INVERSE ($F = 5.84$, $p < 0.0001$), SNR x K ($F = 7.85$, $p < 0.0001$), are all above the significant threshold. Of special interest also the significant interaction between all the main effects SNR x INVERSE x K with a $F = 8.28$ and $p < 0.001$. Correlation values obtained in the left S1 cortical areas for the fMRI-based inverse types (diag-fMRI, corr-fMRI) are statistically significant higher than those obtained for the MN and MNC inverse methods (Scheffe's test, $p<0.005$). This holds for the all range of SNR values studied. In this context, correlation values obtained for the corr-fMRI were higher than those of diag-fMRI. Correlation values decrease significantly for all inverse methods used when data with SNR of 1 or 3 are employed

with respect to the simulations performed with other SNR values (5, 10, 20, 30). Figure 1 presents the mean values obtained for the correlation values in the ROI analyzed when the level of K values and the type of inverse operator were varied. Such interaction between the INVERSE and K main factors is statistically significant($F = 5.84$, $p < 0.0001$). Similar results were obtained for the other ROIs in which fMRI hotspots were present (right M1, SMA).

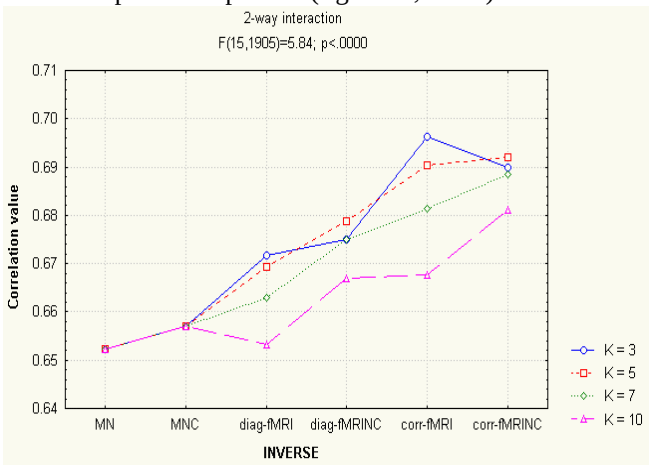

Figure 1. Left S1 area.

B. Left PP region.

Results for this cortical region are here reported as paradigmatic for all the ROIs without fMRI activations used in this simulation (like right S1, M1, and PP areas). All the considered factors (SNR, INVERSE, K) decrease significantly in the simulations the variance of the correlation. F values for SNR ($F = 140.4$, $p < 0.00001$), INVERSE ($F = 33.05$, $p< 0.00001$) and K ($F = 65.5$, $p < 0.00001$) are all above the significant threshold of $p = 0.05$. All the interactions between the main factors of this ANOVA were also significant. F values for K x INVERSE ($F = 65.2$, $p < 0.00001$), SNR x K ($F = 29.06$, $p < 0.0001$), INVERSE x SNR ($F = 25.33$, $p < 0.00001$) are all above the significant threshold. Of special interest also the significant interaction between all the main effects SNR x INVERSE x K with a $F = 29.91$ and $p < 0.0001$. Correlation values obtained in the PP ROI for the fMRI-based inverse types are statistically similar to those obtained for the MN and MNC inverses (Scheffe's test, $p>0.05$). Furthermore, the corr-fMRI performs generally better than diag-fMRI based inverses, for all the level of SNR analyzed. Low values of SNR decrease the value of correlation between the estimated and the simulated waveform in the ROI analyzed, for all methods and level of fMRI priors. The inverse methods that returns higher values for the correlation coefficient in this area are the corr-fMRINC and the MNC, while the best level for the fMRI priors is K = 3. Increasing values of K reduces the correlation values between the estimated and the simulated waveforms. All these observations are statistically significant after Scheffe's post hoc tests performed at the 5% of significance level. Figure 2 presents the mean values obtained for the correlation values in the ROI analyzed when the level of K values were varied. Note the significance of the interaction between the INVERSE and K main factors ($F = 65.2$, $p < 0.0001$).

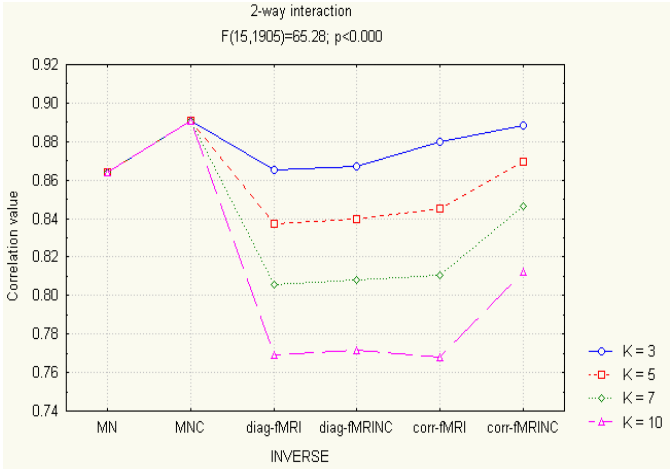

Figure 2. Left posterior parietal area.

IV. Discussion

This simulation integrates the results obtainable by the use of inverse operators performance indexes based on the resolution matrix [2]. This is due to the fact that resolution matrix indexes are valid when no noise is present on the data, a condition rarely met in EEG practice. Results of this simulation suggests that the reconstruction of the cortical currents involving ROIs in which fMRI hotspots are present is better performed by the corr-fMRINC inverse operator (with K = 3 or 5) than the diag-fMRI or minimum norm inverse operators. When the reconstruction was produced for the cortical areas where no fMRI hotspots are present, the performance of corr-fMRI methods (with K = 3) are equivalent to those returned by un- and weighted minimum norm inverse operators. All the inverse methods decrease significantly their performances when the SNR decrease from values of 10, 5 to values of 3 and 1. As result, the use of fMRI-based inverse operators appear to be useful in the reconstruction of cortical current densities from EEG data.

References

[1] Nunez P. *Neocortical dynamics and human EEG rhythms*. New York: Oxford University Press.1995

[2] Babiloni F, Carducci F, Cincotti F, Del Gratta C, Roberti GM, Romani GL, Rossini PM, Babiloni C "Integration of High Resolution EEG and Functional Magnetic Resonance in the Study of Human Movement-Related Potentials", *Method Inform Med* 39: 179–82, 2000.

[3] Dale A, Liu A, Fischl B, Buckner R, Belliveau JW, Lewine J, Halgren E "Dynamic Statistical Parametric Mapping: Combining fMRI and MEG for High-Resolution Imaging of Cortical Activity", *Neuron*, 26: 55-6, 2000.

[4] Shoham D, Glaser DE, Arieli A, Kenet T, Wijnbergen C, Toledo Y, Hildesheim R and Grinvald A.. "Imaging cortical dynamics at high spatial and temporal resolution with novel blue voltage-sensitive dyes". *Neuron* 24: 791–802,1999

[5] Liu AK, Belliveau JW and Dale AM "Spatiotemporal imaging of human brain activity using functional MRI constrained magnetoencephalography data: Monte Carlo simulations", PNAS, 95(15): 8945-50, 1998.